Electronic Supporting Information for

Nickel nanocatalyst within h-BN shell for enhanced hydrogen oxidation reactions

Lijun Gao[a,b‡], Ying Wang[c,‡], Haobo Li[a], Qihao Li[c], Na Ta[a], Lin Zhuang[c], Qiang Fu[a*], Xinhe Bao[a]*

[a]*State Key Laboratory of Catalysis, iChEM, Dalian Institute of Chemical Physics, the Chinese Academy of Sciences, Dalian 116023, P.R. China*

[b]*Department of Chemical Physics, University of Science and Technology of China, Hefei 230026, P.R. China*

[c]*College of Chemistry and Molecular Sciences, Hubei Key Lab of Electrochemical Power Sources, Institute for Advanced Studies, Wuhan university, Wuhan 430072, China*

* Emails: lzhuang@whu.edu.cn; qfu@dicp.ac.cn;

[‡] *Both authors contribute equally*

Experimental Section

Material synthesis

Ni nanoparticles (NPs) supported on commercial carbon (Ketjen Black EC-600JD) were prepared by an impregnation method using $Ni(NO_3)_2 \cdot 6H_2O$ as the precursor. Before impregnation, the carbon support was calcined in air at 350 ^oC for 4 h. The fresh samples were dried in an oven at 120 ^oC overnight, and then reduced in NH_3 at 500 ^oC for 2 h or 700 ^oC for 1 h. The obtained samples were named as Ni/C-500NH_3 and Ni/C-700NH_3, respectively. Alternatively, certain amount of carbon supports and a mixed aqueous solution of $Ni(NO_3)_2$ and boric acid (H_3BO_3) were enclosed into a 100 ml stainless steel autoclave followed by heating at 120 ^oC for 10 h. After cooling to room temperature, the generated solid was dried at 40 ^oC overnight and then annealed at 700 ^oC for 1 h in NH_3. For support-free catalysts, the carbon support was not added for preparing the Ni@(h-BN) core-shell catalysts. The molecular ratio of Ni to H_3BO_3 has been varied between 3:1 and 1:1, and the samples were denoted as Ni_3@$(h\text{-}BN)_1$/C-700NH_3, Ni_1@$(h\text{-}BN)_1$/C-700NH_3, Ni_3@$(h\text{-}BN)_1$-700NH_3 and Ni_1@$(h\text{-}BN)_1$-700NH_3 . The loadings of Ni in the Ni/C-500NH_3, Ni_3@$(h\text{-}BN)_1$/C-700NH_3, and Ni_1@$(h\text{-}BN)_1$/C-700NH_3 catalysts were 27.0%, 32.5%, and 24.2%, respectively, which were measured by inductively coupled plasmas optical emission spectrometer (ICP-OES, 7300DV, PerkinElmer). The three catalysts were treated by microwave digestion before the ICP-OES measurements.

Physicochemical characterization

X-ray diffraction (XRD) patterns were collected on an Empyrean diffractometer using a Cu ka (λ = 1.5406 Å) radiation source and scanning rate of $12^o \cdot min^{-1}$. Transmission electron microscopy (TEM) images were recorded on Hitachi HT 7700 microscope operated at an acceleration voltage of 100 kV, and high-resolution electron microscopy (HRTEM) images were acquired on both JEM-2100 and FEI Technai F30 microscope operated at an accelerating voltage of 200 kV and 300 kV, respectively. Raman measurements were undertaken on a LabRam HR 800 instrument with a 532 nm excitation laser. X-ray photoelectron spectroscopy (XPS) measurements were performed in a Thermo Scientific ESCALAB 250Xi spectrometer using an Al Ka X-ray source and 20 eV pass energy. The C 1s peak located at 284.5 eV was used for calibration of binding energy positions. Infrared

spectroscopic measurement was recorded on Nicolet isso FT-IR spectrometer with a spectral resolution of 4 cm^{-1} accumulating 32 scans. H_2 pulse chemisorption was done using a Micromeritics Chemisorption Analyzer (Auto Chem II 2920). The samples were pretreated in 10% (v/v) H_2-Ar (50 $mL \cdot min^{-1}$) at 210 ^oC for 2 h and then changed to He (50 $mL \cdot min^{-1}$) to purge the chemisorbed hydrogen on samples at 450 ^oC (for Ni/C-500NH_3 catalysts) or 600 ^oC (for Ni@h-BN/C catalysts) for 80 min. After cooling down to 40 ^oC, the samples were exposed to H_2 pulses consisting of 10% (v/v) H_2 balanced with Ar (50 $mL \cdot min^{-1}$). H_2 concentration was measured using a thermal conducting detector (TCD). Temperature-programmed oxidation (TPO) was carried out in a home-made micro-reactor equipped with a mass spectrometer (OMNI STAR). The catalysts were firstly reduced in H_2 (50 $mL \cdot min^{-1}$) at 500 ^oC for 2 h and then cooled down to room temperature in He. The reduced catalysts were heated in 20% (v/v) O_2-He (30 $mL \cdot min^{-1}$) from room temperature to 800 ^oC with a ramping rate of 5 $^oC \cdot min^{-1}$. The products were analyzed by an on-line mass spectrometer.

Electrochemical measurements

Electrochemical experiments were conducted on a CHI-600E potentiostat with a rotating disk electrode (RDE) system (Pine Research Instruments). A sheet of carbon paper (Toray) was used as the counter electrode. The reference electrode was a reversible hydrogen electrode (RHE) in the same solution. 5 mg sample was dispersed ultrasonically in 1 ml diluted Nafion alcohol solution (0.05 wt. %) to form an ink, and the suspension was pipetted onto a RDE with a glassy carbon (GC) substrate (Ø = 5 mm), which was buff-polished with an alumina suspension (Ø = 0.05 μm) prior to use. The catalyst coated electrode was dried under an infrared lamp, and the Ni loading is 0.25 $mg_{Ni} \cdot cm^{-2}$. The hydrogen oxidation reaction (HOR) evaluation was carried out in H_2-saturated 0.1 M NaOH solution with the rotation rate of 2500 revolutions per minute (r.p.m). The potential was scanned from -0.05 V to 0.15 V (vs. RHE) at 5 $mV \cdot s^{-1}$. Cyclic voltammetry (CV) was carried out in N_2-saturared 0.1 M NaOH solution by scanning the potential from -0.05 V to 0.50 V (vs. RHE) at 20 $mV \cdot s^{-1}$. The accelerated durability tests (ADTs) were conducted in 0.1 M NaOH solution by scanning the potential from -0.05 to 0.5 V (vs. RHE) at 100 $mV \cdot s^{-1}$ for 10000 cycles.

Computational details

Density functional theory (DFT) calculations were performed using Vienna ab initio simulation packages (VASP)[1] with the projector-augmented wave (PAW) scheme[2]. The Perdew-Burke-

Ernzerhof (PBE)[3] functional at the level of Generalized Gradient Approximation (GGA) for electronic exchange-correlation interactions has been used. The plane wave cutoff was set to 400 eV. The Brillouin zone was sampled by a 2×2×1 Monkhorst-Pack [4] k-point grid for structural optimizations. The convergence of energy and forces were set to 1×10^{-5} eV and 0.05 eV·Å^{-1}. The weak van der Waals (vdW) interactions were corrected in the form of C^6/R^6 pair potentials (PEB-D)[5], where C^6 for Ni, N, B, H, and O were set to 10.80, 1.23, 3.13, 0.14, and 0.70, and R^{vdW} were set to 1.562, 1.397, 1.485, 1.001, and 1.342, respectively. ΔE_H is defined by: $\Delta E_H = E_{surface+H} - E_{surface} - \mu_H$, and ΔE_O is defined by: $\Delta E_O = E_{surface+O} - E_{surface} - \mu_O$, where $E_{surface+H}$ or $E_{surface+O}$ is the total energy for the surface with adsorbed H or O atoms, $E_{surface}$ is the total energy for the h-BN/Ni surface, and μ_H or μ_O is the chemical potential of H or O with reference to H_2 or O_2: $\mu_H = 1/2\mu(H_2)$, $\mu_O = 1/2\mu(O_2)$. ΔE_{OH} is defined by: $\Delta E_{OH} = E_{surface+OH} - E_{surface} - \mu_{OH}$, where $E_{surface+OH}$ is the total energy for the surface with adsorbed OH groups, $E_{surface}$ is the total energy for the h-BN/Ni surface, and μ_{OH} is the chemical potential of OH groups with reference to H_2O and H_2: $\mu_{OH} = \mu(H_2O) – 1/2\mu(H_2)$.

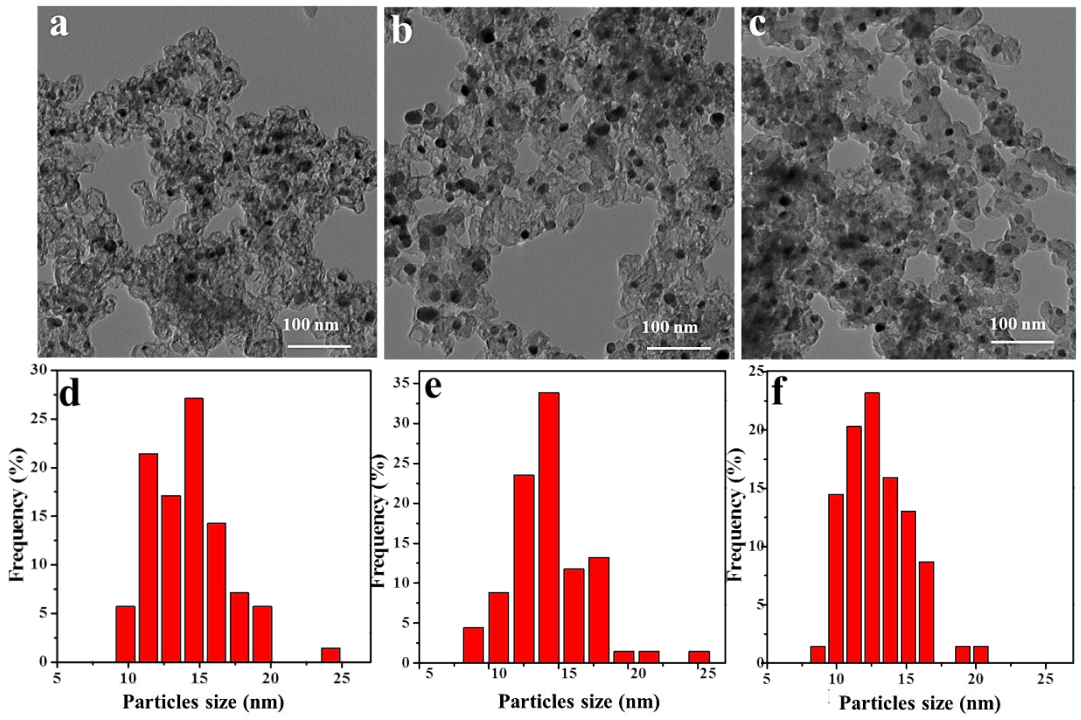

Fig. S1 TEM images and corresponding Ni particles size distributions of Ni/C-500NH_3 (a, d), Ni_3@(h-BN)$_1$/C-700NH_3 (b, e), and Ni_1@(h-BN)$_1$/C-700NH_3 (c, f) samples. The Ni/C-500NH_3 and Ni@h-BN/C samples show uniform size distribution of nanoparticles with an average diameter between 10 and 15 nm. Comparing with Ni/C-500NH_3, Ni nanoparticles in the Ni@h-BN/C catalysts did not sinter although the samples were treated at the higher temperature (700 ^{o}C).

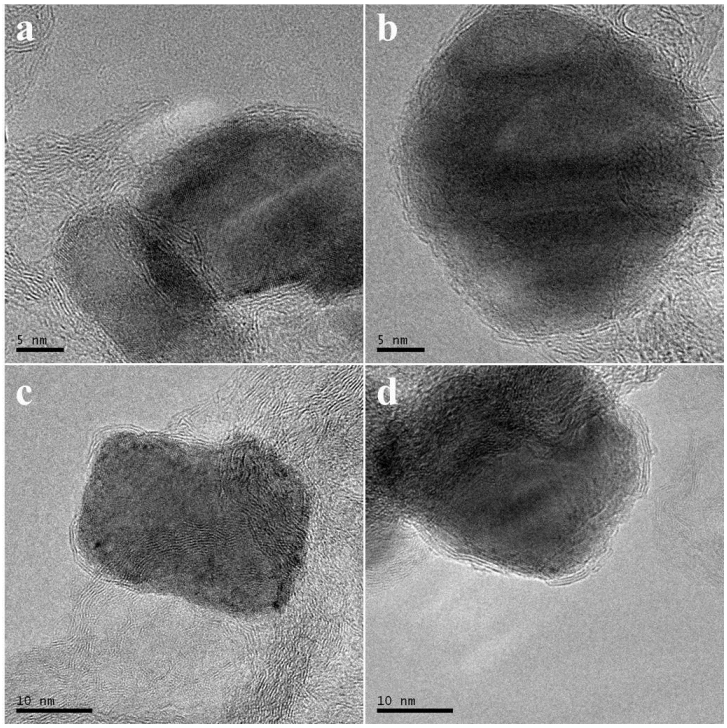

Fig. S2 HRTEM image of the Ni_3@(h-BN)$_1$/C-700NH_3 (a-b) and Ni_1@(h-BN)$_1$/C-700NH_3 (c-d) catalysts. In the Ni@(h-BN)/C samples, the NPs have been covered by graphitic overlayers.

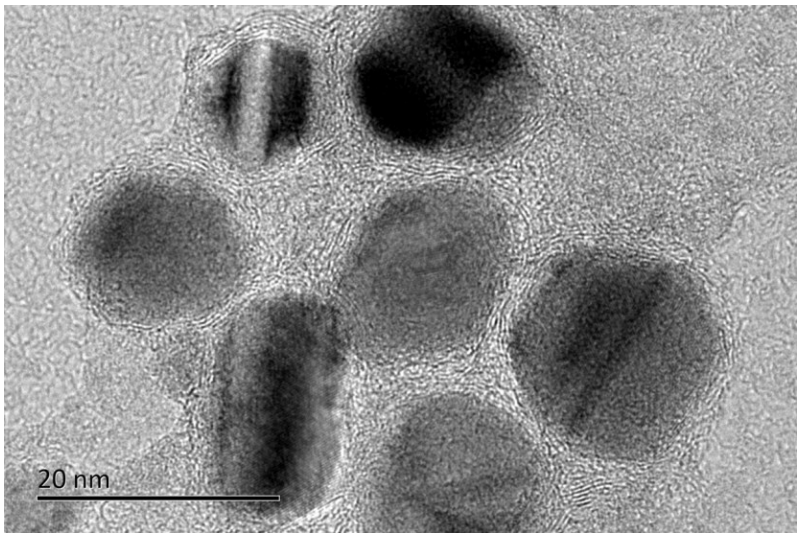

Fig. S3 HRTEM image of the calcinated Ni_1@(h-BN)$_1$/C-700NH_3 catalyst. A Ni_1@(h-BN)$_1$/C-700NH_3 sample was calcinated at 550 ^oC in air to remove the carbon support. The calcinated Ni_1@(h-BN)$_1$/C-700NH_3 catalyst contains similar core-shell nanostructures but the Ni cores were covered by thick and intact h-BN overlayers.

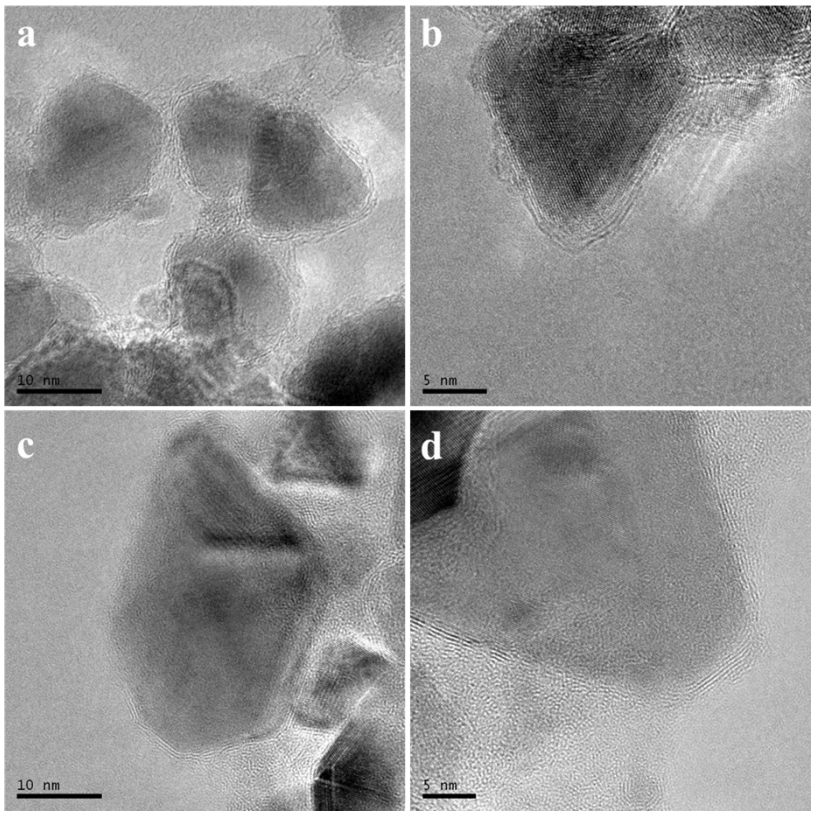

Fig. S4 HRTEM images of support-free Ni_3@(h-BN)$_1$-700NH_3 (a, b) and Ni_1@(h-BN)$_1$-700NH_3 (c, d) catalysts. The support-free Ni@h-BN catalysts were synthesized by the same procedure but without adding the carbon supports.

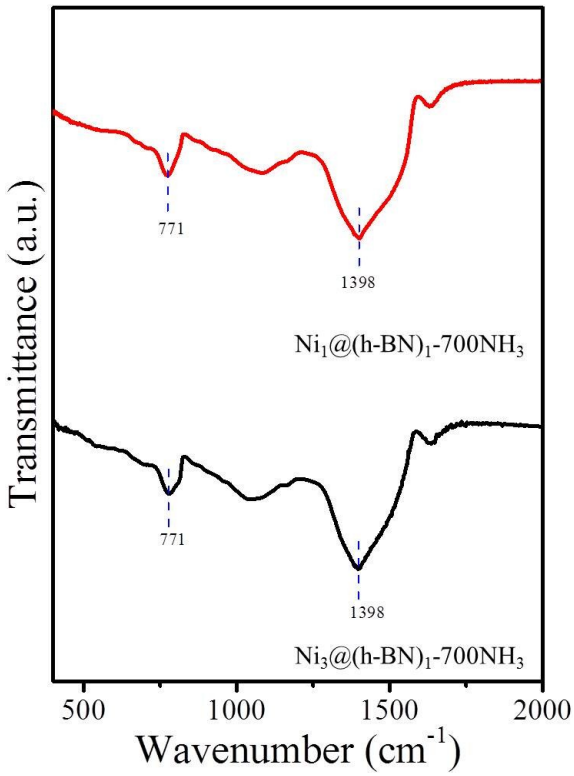

Fig. S5 Infrared spectra recorded from the Ni_3@(h-BN)$_1$-700NH_3 and Ni_1@(h-BN)$_1$-700NH_3 catalysts.

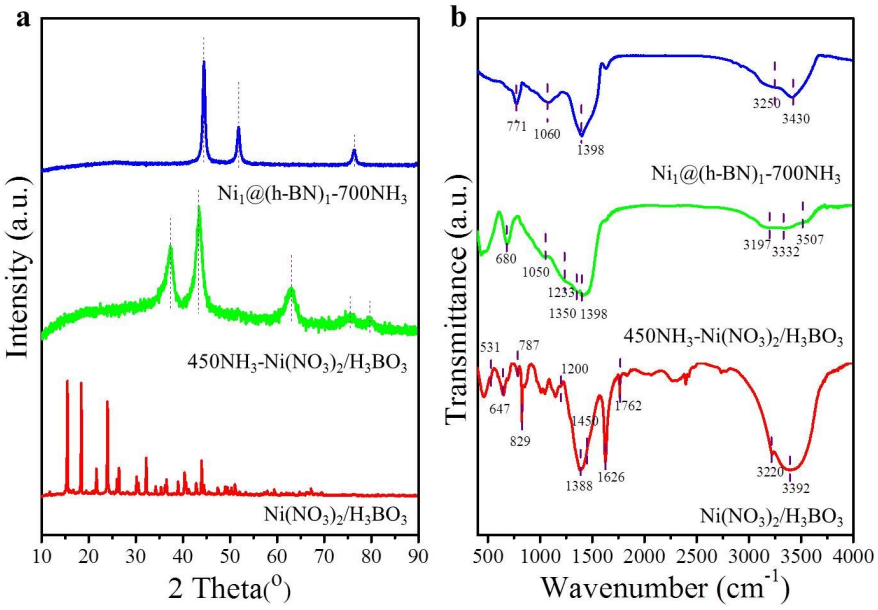

Fig. S6 XRD patterns and IR spectra of $Ni(NO_3)_2/H_3BO_3$, $450NH_3$-$Ni(NO_3)_2$ and $Ni_1@(h\text{-}BN)_1$-$700NH_3$. The XRD patterns show the formation of $Ni(NO_3)_2{\cdot}2H_2O$ (PDF 01-071-1840) after the impregnation. $Ni(NO_3)_2{\cdot}2H_2O$ decomposed to NiO at 450 ^oC and then reduced to metallic Ni at 700 ^oC. In IR spectra, adsorption bands at 1450, 1200, 787, 647, and 531 cm^{-1} can be attributed to B-O, B-O-H, B-O-B, BO_3, and O-B-O groups respectively in the as-prepared sample. The 3220 and 3392 cm^{-1} bands were attributed to O-H and crystal water.[6] The bands at 829, 1388, 1626 and 1762 cm^{-1} were attributed to NO_3^{2-} group from $Ni(NO_3)_2$.[7] After treating by NH_3 at 450 ^oC for 1h, the bands from NO_3^{2-} group disappeared. Meanwhile, boric acid decomposed into boric oxide. The 1233, 1350 and 1398 cm^{-1} was attributed to B-O groups. The 1050 cm^{-1} may be attributed to boron oxynitride species, and 680 cm^{-1} was attributed to BO_3 group. The 3507 and 3332 cm^{-1} were due to NH_2 species, while the 3197cm^{-1} may be due to OH species [6]. When the sample was treated by NH_3 at 700 ^oC for 1 h, the IR spectra show two characteristic peaks of h-BN at 1398 cm^{-1} for in-plane B-N and 771 cm^{-1} for out-of-plane B-N-B. The 1060 cm^{-1} band may be attributed to boron oxynitride species [6]. The XRD and IR spectra results indicated that NH_3 can reduce $Ni(NO_3)_2$ and H_3BO_3 to metallic Ni and h-BN at 700 ^oC after 1 h. The formation of Ni and h-BN happened at the same time.

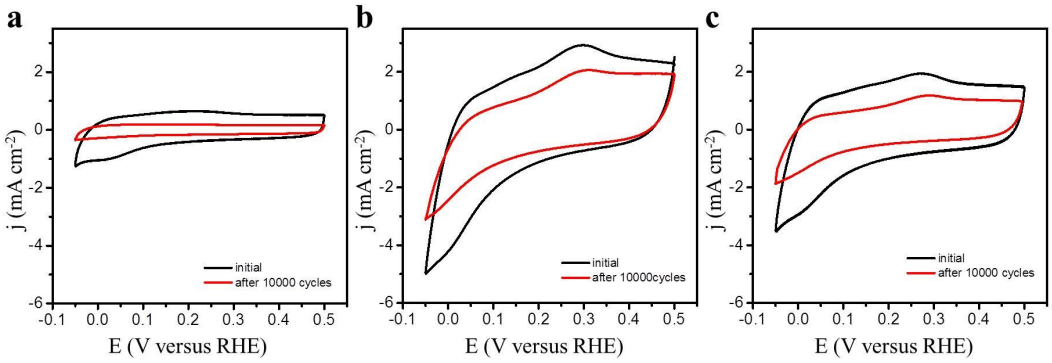

Fig. S7 Cyclic Voltammetry of the (a) Ni/C-500NH_3, (b) Ni_3@(h-$BN)_1$/C-700NH_3, and (c) Ni_1@(h-$BN)_1$/C-700NH_3 samples in N_2-saturated 0.1 M NaOH solution, at 20 mV·s^{-1} before (black) and after (red) ADTs.

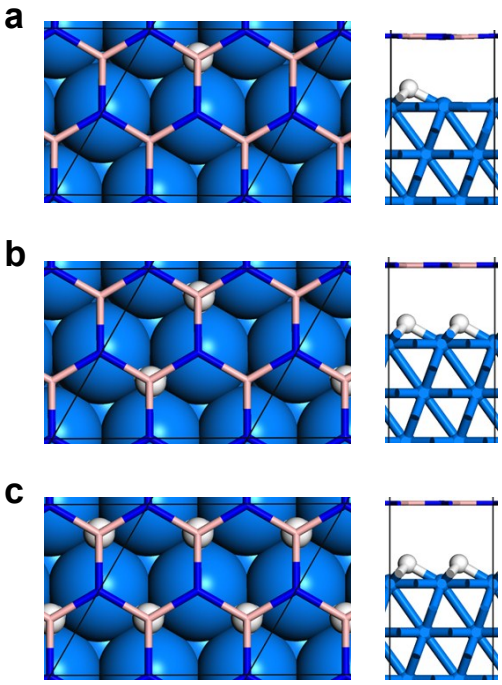

Fig. S8 Atomic structure diagrams of the optimized adsorption structures in figure 4a: H atom adsorption at the interface of h-BN/Ni(111) with the coverage of 1/4 ML (a), 1/2 ML (b), and 1 ML (c).

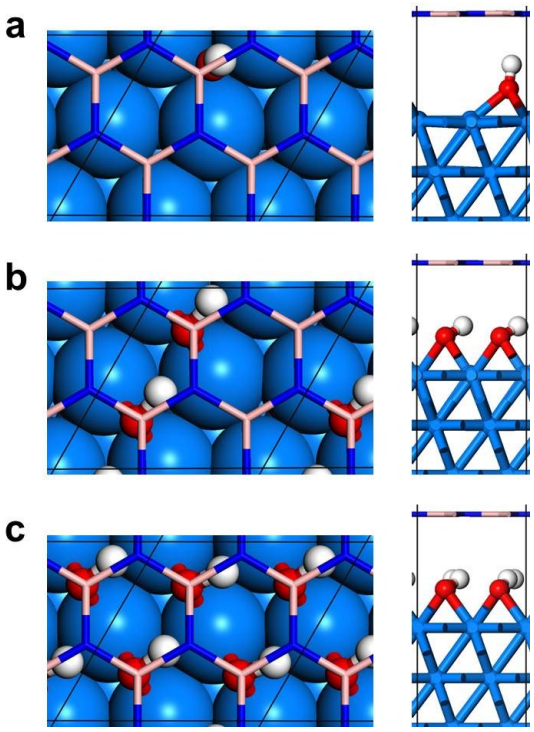

Fig. S9 Atomic structure diagrams of the optimized adsorption structures in figure 4b: OH adsorption at the interface of h-BN/Ni(111) with the coverage of 1/4 ML (a), 1/2 ML (b), and 1 ML (c).

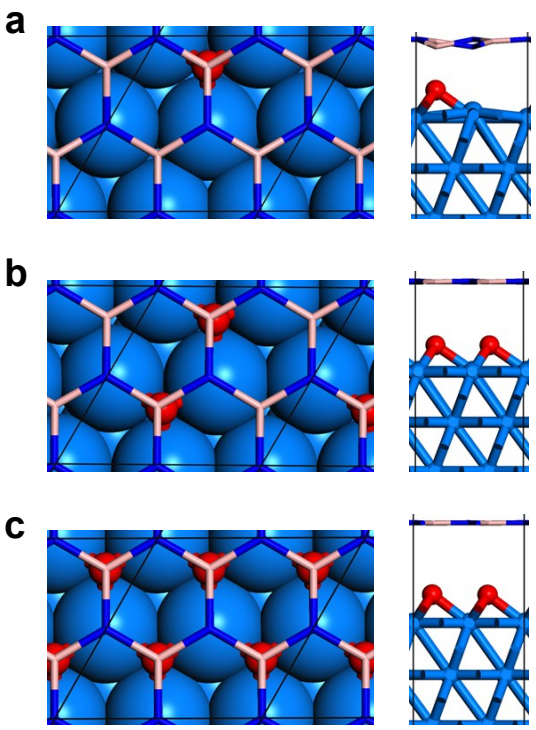

Fig. S10 Atomic structure diagrams of the optimized adsorption structures in figure 4c: O atom adsorption at the interface of h-BN/Ni(111) with the coverage of 1/4 ML (a), 1/2 ML (b), and 1 ML (c).

Reference

1. G. Kresse and J. Furthmüller, *Phys. Rev. B*, 1996, **54**, 11169-11186.
2. P. E. Blöchl, *Phys. Rev. B*, 1994, **50**, 17953-17979.
3. J. P. Perdew, K. Burke and M. Ernzerhof, *Phys. Rev. Lett.*, 1996, **77**, 3865-3868.
4. H. J. Monkhorst and J. D. Pack, *Phys. Rev. B*, 1976, **13**, 5188-5192.
5. S. Grimme, *J. Comput. Chem.*, 2006, **27**, 1787-1799.
6. X. Gouin, P. Grange, L. Bois, P. L'Haridon and Y. Laurent, *J. Alloys Compd.*, 1995, **224**, 22-28.
7. F. Vratny, *Appl. Spectrosc.*, 1959, **13**, 59-70.